OXFORD

Cell-type-specific genes associated with cortical structural abnormalities in pediatric bipolar disorder

Wenkun Lei[1,2,#], Qian Xiao[3,#], Chun Wang[4,#], Weijia Gao[5], Yiwen Xiao[1,2], Yingliang Dai[1,2], Guangming Lu[6], Linyan Su[7] and Yuan Zhong [1,2,*]

[1]School of Psychology, Nanjing Normal University, Nanjing, Jiangsu 210097, China
[2]Nanjing Normal University, Jiangsu Key Laboratory of Mental Health and Cognitive Science, Nanjing, Jiangsu 210097, China
[3]The Mental Health Centre of Xiangya Hospital, Central South University, Changsha, Hunan 410008, China
[4]The Department of Psychiatry, Nanjing Brain Hospital Affiliated to Nanjing Medical University, Nanjing, Jiangsu 210029, China
[5]The Children's Hospital affiliated to the Medical College of Zhejiang University, Hangzhou, Zhejiang 310003, China
[6]The Department of Medical Imaging, Jinling Hospital, Nanjing University School of Medicine, Nanjing, Jiangsu 210002, China
[7]The Second Xiangya Hospital of Central South University, Changsha, Hunan 410008, China
*Correspondence: Yuan Zhong, zhongyuan@njnu.edu.cn
#These authors contributed equally to this work.

Abstracts

Background Pediatric bipolar disorder (PBD) has been proven to be related to abnormal brain structural connectivity, but how the abnormalities in PBD correlate with gene expression is debated.

Objective This study aims at identification of cell-type-specific gene modules based on cortical structural differences in PBD.

Methods Morphometric similarity networks (MSN) were computed as a marker of interareal cortical connectivity based on MRI data from 102 participants (59 patients and 43 controls). Partial least squares (PLS) regression was used to calculate MSN differences related to transcriptomic data in AHBA. The biological processes and cortical cell types associated with this gene expression profile were determined by gene enrichment tools.

Results MSN analysis results demonstrated differences of cortical structure between individuals diagnosed with PBD and healthy control participants. MSN differences were spatially correlated with the PBD-related weighted genes. The weighted genes were enriched for "trans-synaptic signaling" and "regulation of ion transport", and showed significant specific expression in excitatory and inhibitory neurons.

Conclusions This study identified the genes that contributed to structural network aberrations in PBD. It was found that transcriptional changes of excitatory and inhibitory neurons might be associated with abnormal brain structural connectivity in PBD.

Keywords: morphometric similarity; Allen Human Brain Atlas; pediatric bipolar disorder; cell type

Introduction

Bipolar disorder (BD) is a recurrent and chronic disease marked by irritability and emotion swings. Over 1% of the global population carries this diagnosis (Grande *et al.*, 2016).

Compared with adult BD, patients with pediatric bipolar disorder (PBD) demonstrate atypical symptoms, and find it more difficult to achieve remission and prevent recurrence (Goldstein & Birmaher, 2012). BD has high heritability, which some estimate to be as high as 85% (Wray & Gottesman, 2012). Compared to adult BD, PBD patients in probands have a higher risk of transmission to offspring (Oquendo *et al.*, 2013). As a result, PBD is generally considered a more genetically determined distinct subtype of BD (Biederman *et al.*, 2013; Croarkin *et al.*, 2017). Nonetheless, few studies have examined the pathogenesis of PBD.

Research has shown that the prefrontal cortex exhibits weakened control of emotional networks among BD patients, resulting in an abnormally high level of mood and reward processing (Strakowski *et al.*, 2011; Phillips & Swartz, 2014). Findings from recent neuroimaging studies pointing to reduced cortical volume in brain areas such as the anterior cingulate cortex (ACC) and insula

among BD patients could offer an explanation for this (Bora *et al.*, 2010; Selvaraj *et al.*, 2012).

Two traditional methods, tractography based on diffusion-weighted imaging (DWI) (Forde *et al.*, 2015) and structural covariance network (SCN) analysis (lexander-Bloch *et al.*, 2013), have gained widespread application in investigating BD brain anatomical connectomes. Diffusion imaging studies have indicated widespread changes in PBD patients with regards to the anatomical connection of cortical networks (Fernandes *et al.*, 2019). However, DWI tractography is still controversial in terms of precision, particularly when computing connectivity strength of long-distance projections (Donahue *et al.*, 2016; Maier-Hein *et al.*, 2017). SCN analysis has indicated significant alterations relating to BD (Han *et al.*, 2020; Kim *et al.*, 2020). However, the accuracy of SCN analysis is subject to sample size, and this method cannot be applied to individual analysis in most cases. Furthermore, the biological interpretation of SCN analysis results is still in dispute (Alexander-Bloch *et al.*, 2013).

Therefore, a new similarity-based approach—morphometric similarity network (MSN) analysis—has recently been put forward

and tested to reveal macroscale cortical organization (Seidlitz *et al.*, 2018). MSNs harbor a powerful toolset to reveal macroscale cortical organization. It is characterized by capturing correlation between regions of various morphological features in multiple forms for one individual. In cytoarchitectonics, growing evidence shows that closely connected cortical regions exhibit high levels of coexpressed genes, and often share the same cytoarchitectonic class. What is more, nodes with similar histology are more inclined to be axonally connected between cortical areas (Goulas *et al.*, 2017; Wei *et al.*, 2019). Compared with DWI-based networks and SCN, MSNs have the highest proportion of intra-class edges. This suggests that edges in MSNs are more likely to be representational of pairings of regions with similar histology and a propensity for axonal connectivity, and have stronger connections with genomic and cytoarchitectonic classes than in SCNs and DWI networks (Seidlitz *et al.*, 2018). MSN could thus shed light on the gene expression and cellular architecture underlying structural network abnormalities in patients with PBD. Recent studies have demonstrated that transcriptomic and cellular information of brain regions subject to neuropsychiatric disorders could be revealed through alterations in MSN. However, MSN has not yet been applied to reveal brain morphological differences in PBD patients.

In neuroimaging-genetics studies, intermediate phenotypes have potential scientific value as genetic markers in relation to clinical measures (Walton *et al.*, 2013). For BD specifically, ankyrin-G protein (ANK3) and calcium channel, voltage-dependent, L type, and alpha 1C subunit (CACNA1C) were linked to certain functional and anatomical neuroimaging phenotypes (Lippard *et al.*, 2017; Ou *et al.*, 2015). With connectome and molecular imaging developing, researchers discovered a method for interrogation of neuronal connection across the human brain through genetics (Arnatkeviciute *et al.*, 2021; Fornito *et al.*, 2019). The Allen Human Brain Atlas (AHBA) provides a distinct perspective to comprehend how variations in gene expression associate with neuroimaging phenotypes on a macroscopic level (Fornito *et al.*, 2019). Recent research combined structural indicators (Anderson *et al.*, 2020; Li *et al.*, 2021) of mentally disabled patients with data on AHBA expression to reveal dysregulation of cell levels.

In this study it is hypothesized that: (i) structural dysconnectivity in PBD could be tested by MSN; (ii) the structural network phenotype is related to structurally patterned transcriptomic data in AHBA; and (iii) the genes most strongly associated with morphometric similarity differences in case-control (PBD-HC) were enriched. To test this, MSNs were constructed to describe the PBD-related structural abnormalities in two independent cohorts. Partial least squares (PLS) regression was utilized to acquire the clusters of weighted genes based on the association between MSN alteration and AHBA data. The enrichment pathways and cell types were obtained from the weighted genes.

The study aims to determine PBD-related MSN alterations and related genes to uncover the cellular and molecular mechanisms behind MSN changes in PBD.

Method

Participants for neuroimaging analysis

All performed methods met the standards of ethics set by the Xiangya Hospital and the National Research Council of China and the specifications in the Declaration of Helsinki (1964). The study involved 102 individuals (59 patients and 43 healthy control participants) at the Pediatric Psychiatry Clinic of Changsha Xiangya Second Hospital, Hunan province (59 patients and 20 healthy con-

trol participants), and the Nanjing Brain Hospital Affiliated to Nanjing Medical University in Jiangsu (23 healthy control participants). Participants were all fully informed of the procedures and their guardians all provided signatures to consent forms.

In this study, PBD patients met the DSM-V BD standard criteria for diagnosis. The following exclusion criteria were designed for individuals with PBD: (i) age under 10 or over 18; (ii) other concurrent psychiatric conditions; (iii) physical illness that causes a mental disorder; (iv) pregnancy; (v) use of illegal substance abuse within 60 days before being admitted; and (vi) other specified bipolar spectrum disorder and BD not otherwise specified. Participants in PBD group who had an episode of mania or hypomania and those diagnosed with euthymic PBD with >1 month of remission were also included. In total, 59 adolescent patients were eligible for this study.

The exclusion criteria for control group participants were as follows: (i) current or history of psychiatric diagnosis; (ii) a history of psychiatric diagnosis in a first-degree relative; (iii) sustained physical and neurological conditions; and (iv) currently pregnant.

The Adolescent Mania Scale (YMRS) (Young *et al.*, 1978), Mood and Feelings Questionnaire (MFQ) (Wood *et al.*, 1995), and Pittsburgh Sleep Quality Index (PSQI) (Buysse *et al.*, 1989) were used to assess the severity of emotional symptoms for each participant. All evaluations were conducted on the same day as the MRI scan.

MRI data acquisition

For the MRI scan, all participants were told to relax and remain motionless with eyes closed but stay awake. Foam padding was used to reduce head motion. All MRI data from the participants were acquired from a 3T Siemens scanner at the Magnetic Resonance Center at Hunan Provincial People's Hospital and Nanjing Brain Hospital Affiliated to Nanjing Medical University. The regular axial three-dimensional T1-weighted (T1w) images were captured by a spoiled gradient recall sequence. The following were the T1w scan parameters: slice thickness = 1.0 mm, gap = 0 mm, echo time (TE) = 2.03 ms, repetition time (TR) = 2300 ms, flip angle = 9°, FOV = 256 × 256 mm^2, matrix = 256 × 256, and slices number = 176. Subsequently, the DTI images were obtianed by performing a single-shot echo planar imaging (EPI) sequence aligned with the anterior–posterior commissure line. Integral parallel acquisition technique (iPAT) was applied with an accelerate factor of 2.45 continuous axial slices completed in 12 min and 56 s. The diffusion sensitizing gradients involved the baseline image with no diffusion weighting ($b = 0$ s/mm^2) along with diffusion-weighted images ($b = 1000$ s/mm^2) along 30 nonlinear directions. There were the following imaging parameters: TR = 6100 ms, TE = 93 ms, slice thickness = 3 mm, gap = 0 mm, FOV = 240 × 240, acquisition matrix size = 128 × 128.

Data preprocessing

FreeSurfer (v.7.2, http://surfer.nmr.mgh.harvard.edu/) was applied for preprocessing and analyzing the three-dimensional T1w images. The original T1w data was processed by skull stripping, brain tissue segmenting, separating hemispheres as well as subcortical structures, and constructing the white or gray interfaces as well as pial surfaces to reconstruct the cortical surface. We preprocessed DTI data using FMRIB's Diffusion Toolbox, which is implemented in FSL 6.04 (http://www.fmrib.ox.ac.uk). Each DWI was affine aligned to $b = 0$ to correct the motion artifacts and the eddy current-induced distortion. The brain extract toolbox was used to remove skull components from the images. Diffusion tensors were fitted with linear least squares and eigenvalues were

decomposed to determine the fractional anisotropy and mean diffusion.

Participants were disqualified if they had bad quality images. Exclusion criteria included failure of full cortical coverage during the DTI scan, poor registration from the DTI image to the T1w image, or failure of FreeSurfer surface segmentation.

The MSN Processing Pipeline

A multimodal imaging parcellation that had a division to laminate cortical features into 360 regions on biological basis (Glasser *et al.*, 2016) was used on Fsaverage template's surface. This parcellation was modified to fit surface of each participant to create an individual surface parcellation. Then, the parcellation was adjusted and expanded to the individual DTI volumes. For each region, seven morphometric parameters (Seidlitz *et al.*, 2018) (gray matter volume, surface area, cortical thickness, mean curvature, intrinsic curvature, fractional anisotropy, and mean diffusion) were extracted from T1w images and DTI images (Supplementary Fig. S1, available online).

To account for scanner differences, ComBat harmonization (Yu *et al.*, 2018) was utilized to correct the site's effects on the morphometric indies across scanners and sites.

The seven morphological features of each region were then *z*-normalized. Pearson's correlational analysis was performed between each paired cortical region to generate a 360 regions × 360 regions morphometric similarity matrix for each participant. Subsequently, these matrices (360 regions × 360 regions) were calculated by Pearson correlation between regions of these seven features to obtain a 360 × 360 morphometric similarity matrix (Supplementary Fig. S2) (Morgan *et al.*, 2019; Seidlitz *et al.*, 2020).

Case-control differences in MSN

A regional MSN value for each cortical region was calculated by averaging weighted correlation coefficients in the 360 × 360 matrices across the 360 cortical regions (Supplementary Fig. S1). General linear models (GLM) with covariates including education, sex, and age were used to estimate case-control differences. A PBD-HC alteration map was obtained with a two-sided *t*-value that compared PBD and healthy control participants in all regions. The P value was obtained by a permutation test (10 000 times) with significance set at $P < 0.005$ with false discovery rate (FDR) correction for multiple comparisons across 360 regions.

Gene expression data

We utilized the AHBA dataset to obtain brain gene expression taken from six post-mortem adult brains (Sunkin *et al.*, 2013). The AHBA covered almost the whole brain, which consisted of expression measurements of 20 737 genes with detection made by 58 692 probes extracted from 3702 distinctive tissue samples (Arnatkeviciute *et al.*, 2019). Several other procedures were performed to correlate the expression measurements and the neuroimaging data, and can be summarized into seven steps: (i) testing probes to genes for accurate annotations; (ii) filtering probes from background noise; (iii) selecting specific probes to index expression genes; (iv) assigning tissue samples from the AHBA to HCP_MMP1.0 parcellation (360 distinct areas); (v) accounting for individual differences by normalized measure; (vi) filtering inconsistently expressed genes in six brains based on differential stability; and (vii) explaining the spatial effects in gene expression. Since the AHBA data set contains only two data from the right hemisphere, this study only extracted data from the left hemi-

sphere. The resulting matrix depicted transcriptional levels from 10 027 gene expression levels × 177 areas (Fig. 1A).

Transcription-imaging association utilizing PLS regression analysis

The next step involved application of PLS regression to determine genes significantly related to MSN alterations (Krishnan *et al.*, 2011). The gene expression data of 177 regions were taken as independent variables, and the *t*-values of the 177 regions in MSN alterations were set as dependent variables. The PLS components were ranked via the explained variance between predictive and response variables. Furthermore, the PLS regression components (PLS1) that came out first were the most highly correlated with regional variations in MSN. A spatial permutation test (5000 times) was used to verify whether the PLS1 was statistically significant (Vasa *et al.*, 2018). To estimate each gene's variability within PLS1, bootstrapping was applied. By calculating the weight of each gene to the standard bootstrap error of this gene, a Z value was produced, and the genes were ranked based on their contribution to PLS1 (Morgan *et al.*, 2019). Significant genes were chosen with positive (PLS+) and negative weights (PLS−) (Romero-Garcia *et al.*, 2019) or FDR of 5‰.

Analysis of PBD-related genes from previous study

We selected the PBD associated genes from the previous study (Dimick *et al.*, 2020), which provided a summary of existing literature of the genetics in early-onset BD. This summary contained 31 genes that have been relevant to early-onset BD. The identified genes included: DRB2, ANK3, BDNF, CACNA1C, COMT, DRD1, DRD2, DRD3, DRD4, EGR3, GAD1, GSK3B, GSTM1, GSTT1, GSTZ1, HTR2A, HTR2C, MAOA, MCP1, NR1D1, PER3, RORB, SLC6A3, SLC6A4, SNAP25, TH, TPH2, TRL2, TRL4, TRPM2, and XBP1 (31 genes).

Overlapping genes were obtained from the 31 identified PBD-related genes and the 10 027 background genes. This step was performed to explore how PBD-related genes contributed to the PLS analysis. The expression of these overlapping genes on average was obtained from scores of PBD-related gene expression in all samples. Pearson's correlational analysis was used to investigate how the expression levels of PBD-related genes were associated with the MSN *t*-maps. To examine whether the correlation was significant, permutation testing was subsequently used along the same pipeline, and genes in each of the 10 000 permutations were selected in a random manner. This step was for assessment of the significance of the resulting correlation. The significance threshold was chosen at $P < 0.05$ with FDR correction.

We used the gene sets based on post-mortem brain matter measurements of messenger RNA from case-control analysis to test the enrichment of up-/down-regulated genes in BD (Gandal *et al.*, 2018). A resampling procedure was set by 10 000 randomly chosen brain-expressed gene sets. Gandal *et al.* (2018) also included lists of up- and down-regulated genes in the brain in other major psychiatric disorders involving major depressive disorder, schizophrenia, autism spectrum disorder, and alcoholism. The enrichments were also tested based on the neighboring disorder in the same pipeline. The significance level was set at $P < 0.05$ with FDR correction.

Gene functional annotation

The PLS1 gene list ($Z < −5$ or $Z > 5$) was entered into Metascape. Metascape (Zhou *et al.*, 2019) was used to obtain the gene ontology
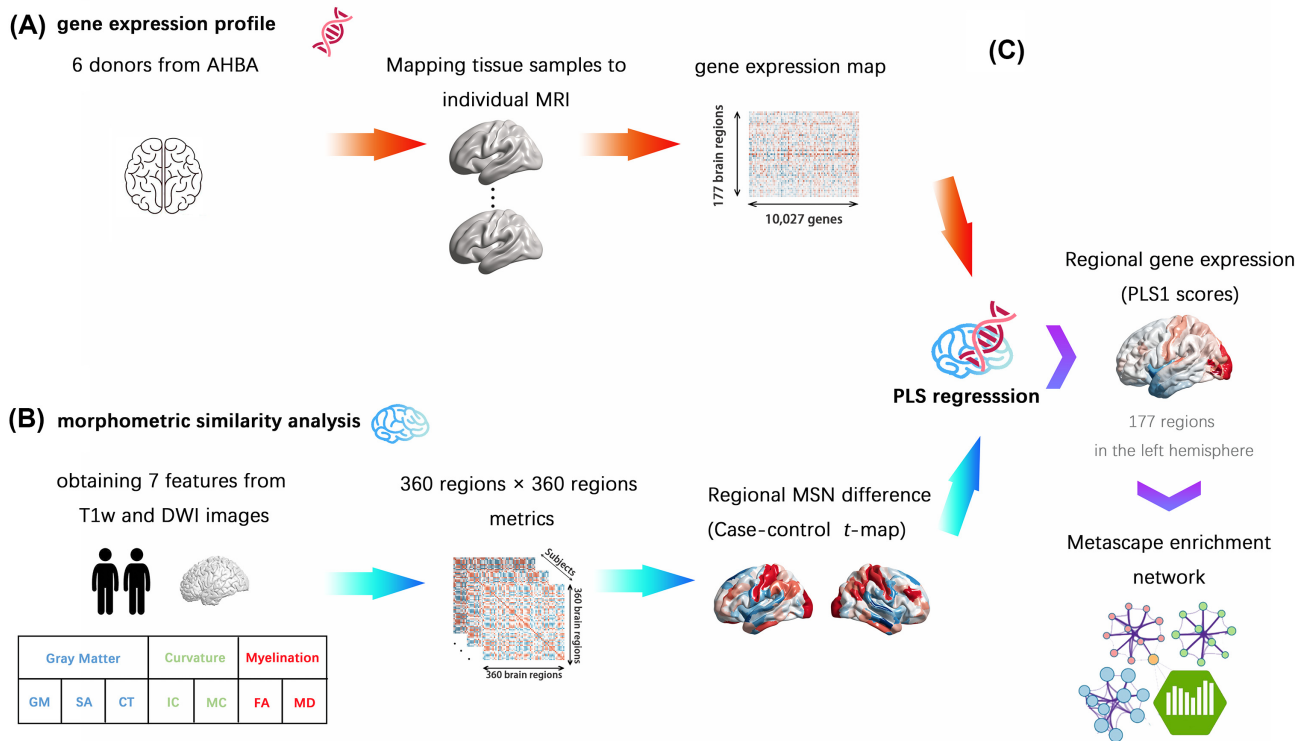
Figure 1: Preview of the procedure. (A) Gene expression profiles. Gene expression profiles in 177 regions (only left hemisphere), which were acquired from the AHBA, were mapped into gene expression maps (177 regions × 10 027 genes). (B) MSN analysis. MRI data, including seven morphometric features, was calculated into metrics (depicted by a HCP's neuroimaging approach, –360 regions × 360 regions). Subsequently, the regional MSN difference (case-control t-map) was computed. (C) PLS regression. PLS regression was used for identification of the associations between imaging and gene expressions and for obtaining the related gene list. This step was followed by performance of enrichment analysis on the gene list.

(GO) gene sets (Ashburner *et al.*, 2000) that assisted with determining biological processes.

Identification of cell type specificities for MSN changes

To determine gene sets from each cell type, we used the datasets based on five distinct single-cell studies of the adult human cortex to assign the PLS1 genes to seven specific cell types (Darmanis *et al.*, 2015; Habib *et al.*, 2017; Lake *et al.*, 2018; Li *et al.*, 2018; Zhang *et al.*, 2016). According to the procedure in a previous study (Seidlitz *et al.*, 2020), specific cell types included oligodendrocyte precursors, excitatory neurons, inhibitory neurons, endothelial cells, microglia, astrocytes, and oligodendrocytes. This method avoided bias regarding acquisition error analysis as well as thresholding, and obtained gene sets from each cell type (Seidlitz *et al.*, 2020).

Results

Sample characteristics

The clinical and demographic data from the participants are presented in Table 1. No statistical differences were found between these groups in age, gender, or education.

PBD-related changes in MSN

The case-control (PBD-HC) t-map was obtained through performing a linear regression with sex, education, and age as covariates. The subsequent step was extraction of the two-sided mean t-statistical value, which compared PBD patients with healthy

control participants in all regions (Fig. 1A). Increased and decreased MSN values imply less or more morphometric similarities between these regions and other areas of the cortex. Compared with healthy control participants, patients with PBD were found to exhibit decreased MSN weights in the left superior temporal gyrus, dorsomedial prefrontal cortex, anterior cingulate, midcingulate cortex, right dorsomedial prefrontal cortex, posterior cingulate cortex, and superior temporal gyrus. Increased MSN weights were found in the left lateral occipital cortex, orbital frontal cortex, postcentral gyrus, right lateral occipital cortices, postcentral gyrus, and dorsolateral prefrontal cortex (Fig. 2A, all $P_{FDR} < 0.005$; Supplementary Table S1 available online).

Regarding the Adolescent Mania Scale (PSQI), YMRS, and the MFQ, there was no significant correlation among these clinical variables (Supplementary Table S2).

Gene expression relevant to MSN alteration

PLS regression was applied to determine differences in gene expression of 10 027 genes and regional MSN (177 regions) in the left hemisphere (Fig. 1C). The first component (PLS1) captured the largest fraction (explained 23% of the variance with spatial permutation test, $P_{spin} < 0.001$; Fig. 2B) of all gene expression variances across cortical regions. Furthermore, significant correlation was found between the PLS1 weighted map and the t-map (Pearson's $r_{(177)} = 0.48$, $P < 0.0001$; Fig. 2B). Next, 733 PLS+ positively weighted genes ($Z > 5$) and 507 PLS− negatively weighted genes ($Z < −5$) were filtered from the threshold $Z > 5$ or $Z < −5$, because they were under-expressed (over-expressed) as decreased (increased) regional variations in MSN. All genes underwent FDR

Table 1: Clinical and demographic characteristics.

	PBD (n = 59)	HC (n = 43)	P values
Gender (male/female)	29/30	13/30	0.087[b]
Age (years)	15.02 (1.78)	15.58 (2.25)	0.165[a]
Education (years)	8.10 (1.78)	8.86 (2.46)	0.078[a]
YMRS scores	14.19 (13.98)	-	-
MFQ scores	13.58 (12.37)	-	-
PSQI scores	6.20 (3.59)	-	-
BD-I/BD-II	36/23	-	-
PBD-manic	21	-	-
PBD-depression	17	-	
PBD-remitted	21	-	-
Onset age (years)	13.73 (1.82)	-	-
Illness duration (months)	16.25 (13.70)		
Familial BD history (yes/no)	14/45	-	-
Psychotic symptoms (yes/no)	31/28	-	-
Medications			
Lithium	20	-	-
Valproate	28	-	-
Atypical antipsychotics	39	-	-
Antidepressants	4	-	-

Note: Means are presented in the table (standard deviations). Abbreviations: HC, healthy control participants; "[a]", the two-sample *t*-test (two-sided). "[b]", the Chi-square test. "*" indicates $P < 0.05$.
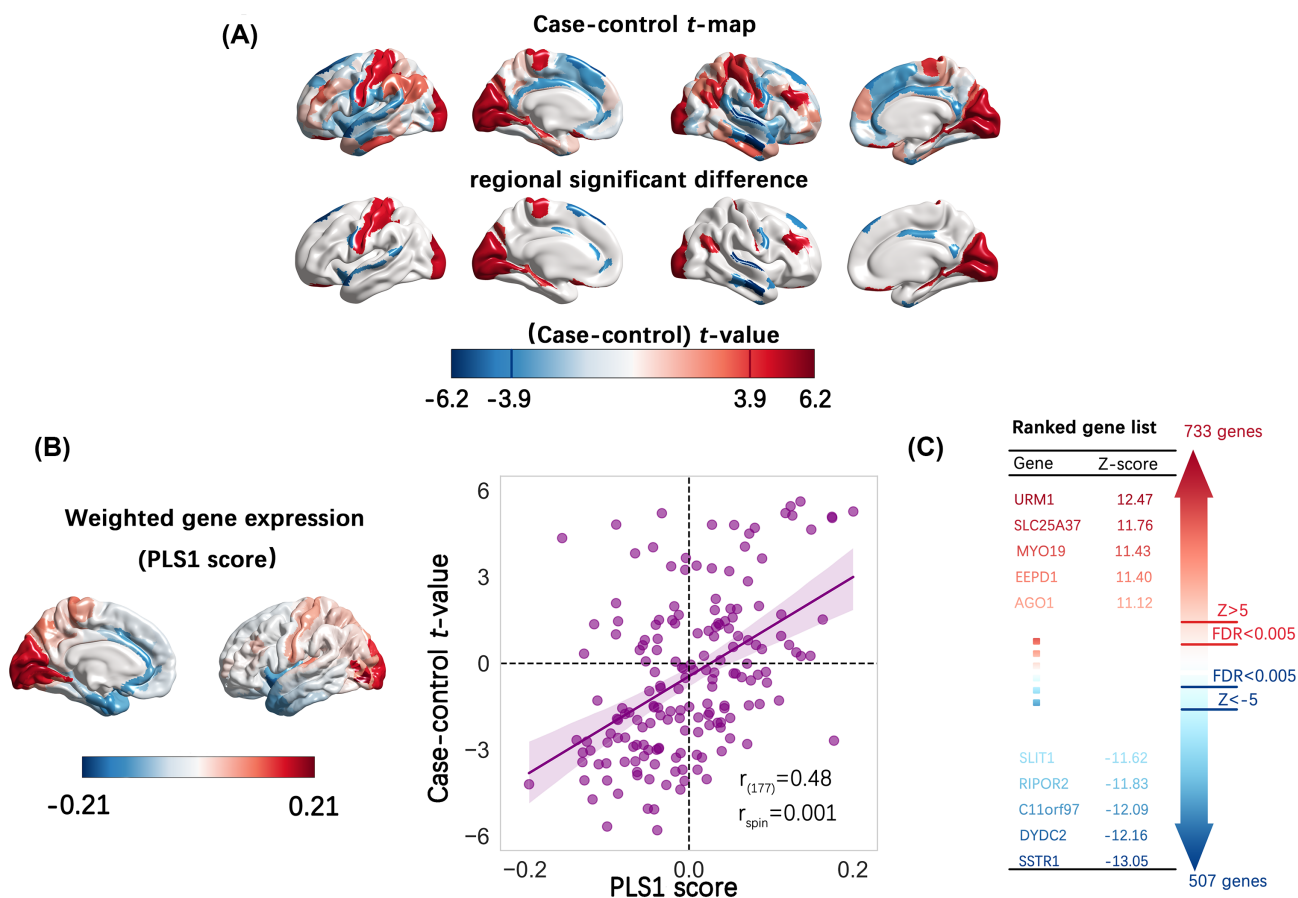

Figure 2: Case-control differences in MSN and the association between the related gene expression and differences in MSN. (A) Case-control differences (*t*-map) in MSN. Higher/lower values in PBD are presented as warm/cold colors (*t*-value > 3.9, $P < 0.005$ corrected by FDR). (B) Gene expression profiles for PLS1, and the scatterplot show the correlation between PLS1scores (a weighted sum of 10 027 gene expression scores) and regional differences in MSN ($r_{(177)} = 0.48$, $P_{spin} < 0.001$). (C) Ranked gene list.
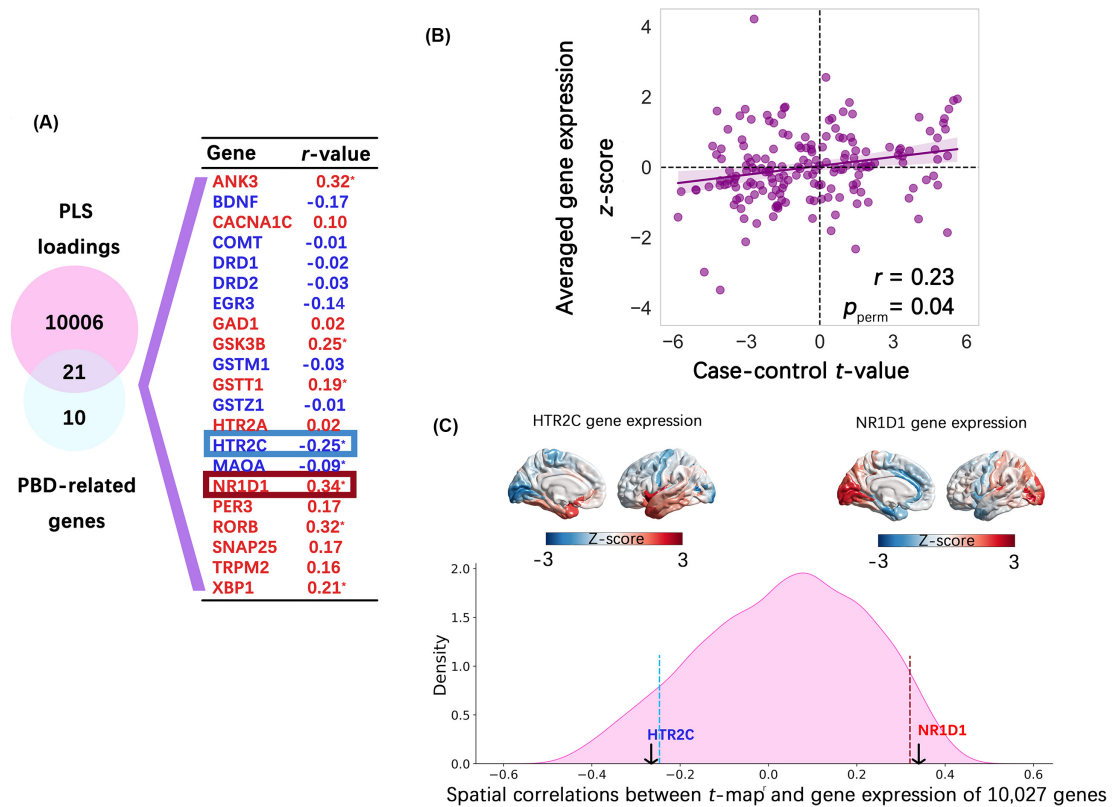
Figure 3: The association between the related gene expression and morphometric similarity differences. (A) The overlapped PBD-related genes from meta-analysis positively and negatively (all r values were calculated with Pearson correlation) correlated with case-control differences. All P value have been corrected by FDR, "∗" indicated the $P < 0.05$ by FDR corrected. (B) Scatter plots demonstrating how the average PBD risk gene expression associated with t-map using Pearson's correlation. Permutation test (21 randomly selected genes replacing risk genes; 10 000 permutations) based P values were provided. (C) Spatial correlation distribution (Pearson's correlation) of t-map and gene expression profiles extracted from the left hemisphere ($n = 10 027$), with NR1D1 (Nuclear Receptor Subfamily 1 Group D Member 1) and HTR2C (5-Hydroxytryptamine Receptor 2C) being most significant. The top 5% and bottom 5% significant genes were separated by a dashed line in the whole gene sets.

correction with $P < 0.005$ (Fig. 2C). Twenty-one overlapping genes were obtained from the 31 selected PBD-related genes and 10 027 background genes. The results showed significant associations ($r = 0.29$, $P_{perm} = 0.01$, permutation times = 10 000; Fig. 3B) between the average PBD-related gene expression and MSN t-maps. Ten of 21 PBD-related genes were found to significantly correlate with regional MSN differences ($P_{FDR} < 0.05$; Fig. 3A), involving six positive correlations (ANK3, GSK3B, GSTT1, NR1D1, RORB, XBP1) and two negative correlations (HTR2C, MAOA). NR1D1 displayed the highest degree of positive correlation in the list, while HTR2C displayed the highest degree of negative correlation (Fig. 3C). Details about the correlations are provided in Supplementary Table S3.

PLS− genes were found to be significantly enriched for the down-regulated Gandal *et al.* (2018) genes (permutation test $P = 0.010$, FDR corrected). PLS1 enrichments in up-/down-regulated gene sets across other psychiatric disorders were also observed (Supplementary Table S4).

Enrichment analysis

The enrichment analysis for the PLS− gene list ($Z < −5$, including 755 genes) revealed the top 10 GO biological processes that showed significance, including "trans-synaptic signaling", "modulation of chemical synaptic transmission", and "regulation of ion transport" as examples (Fig. 4A, B). The equivalent results for PLS+ genes are also provided in the Supplementary Material (Supplementary Table S4, Fig. S1).

Specific cell types for MSN differences

The PLS− genes yielded significant specific expression in excitatory neurons (count = 67, $P_{perm} = 0.01$, adjusted by FDR correction) and inhibitory neurons (count = 51, $P_{perm} = 0.01$ adjusted by FDR correction, Fig. 4C). To further refine the analysis, the enrichment analysis was performed for the gene expression of seven cell types, revealing the alterations in MSN of individuals with PBD (Fig. 4B). The enrichment results for GO terms in neuronal cells included "regulation of regulation of synapse assembly", "response to alcohol", and "regulation of transmembrane transport" (Fig. 4B). The PLS+ genes were not significantly involved in any cortical cell type.

Discussion

In this study, spatial correlations between MSN t-map differences and gene expression were analyzed for individuals with PBD-related abnormalities. To further investigate specific cortical cell types enriched for MSN alteration, we mapped the weighted genes to biological processes that were associated with neuronal cells. The results might contribute to further understanding of cellular and molecular mechanisms within PBD.

MSNs that incorporate information from several cortical parameters in an individual might reveal the structural connections between various brain regions based on axonal connectivity and histological similarity inside a particular human brain. Decreased morphometric similarity was observed in
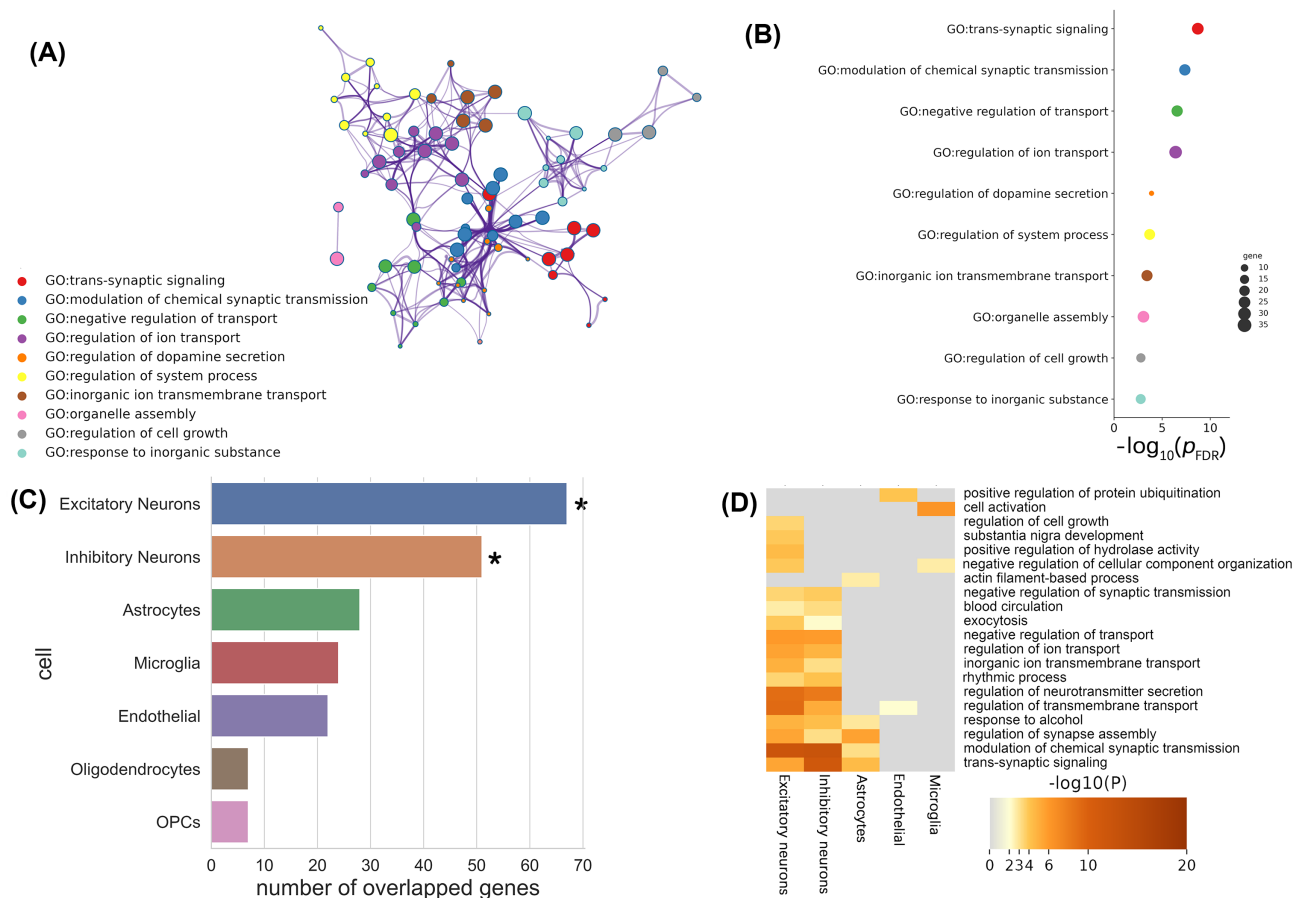
Figure 4: PLS− genes enriched and assigned to cell types. (A) Metascape enrichment network visualization of GO biological processes obtained from PLS1− genes list ($Z < -5$). (B) Ontology terms for PLS1− genes list ($Z < -5$), the size of circle node is proportional to the number of genes in each term. Color represents the different clusters. (C) Gene expression profiles of all cell types with overlapped genes in PLS1− gene list and cell type-specific genes (astrocytes, endothelial cells, microglia, excitatory neurons, inhibitory neurons, oligodendrocytes, and oligodendrocyte precursors). (D) The barplot of the count of overlapping genes for all the cell types (excitatory neurons: count = 67, $P_{perm} = 0.01$; inhibitory neurons: count = 51, $P_{perm} = 0.01$; astrocytes: count = 28, $P_{perm} = 0.99$; endothelial: count = 22, $P_{perm} = 0.99$; microglia: count = 24, $P_{perm} = 0.81$; oligodendrocyte precursors (OPCs): count = 7, $P_{perm} = 0.81$; oligodendrocytes: count = 7, $P_{perm} = 0.99$). All P values have been adjusted by FDR.

the cingulate cortex, temporal lobe, and dorsomedial prefrontal regions for PBD group. It suggests reduced architectonic differentiation and lower axonal connectivity between the previously mentioned cortical regions, as well as a weakening of the linkages between them at the histological and cytoarchitectonic levels. Our findings were consistent with several studies reporting reduced gray matter volume and cortical thickness in the temporal lobe, cingulate cortex, and medial prefrontal cortex in BD (Brooks *et al.*, 2011; Gong *et al.*, 2021; Zhang *et al.*, 2022). The medial prefrontal cortex is vital to emotion generation and regulation through its connection with subcortical areas (Anticevic *et al.*, 2013; Brooks *et al.*, 2011). The anterior and midcingulate cortical regions are important for emotion because they carry out the instrumental, goal-directed behaviors that are brought on by emotions. Therefore, impairment in the anterior cingulate areas does affect mood (Rolls, 2019). The temporal lobe, the part of the brain connected to hearing and vision, is essential for processing emotions and working memory (Antonius *et al.*, 2011). We therefore speculated that decreased axonal connectivity in the previously mentioned regions causes a disturbance in the emotional circuitry, which impairs the emotional control function of patients with PBD. Additionally, the PBD-related increase in MSN was found to compile in "von Economo secondary sensory" systems (Koskinas). This system's main functions are concentrated in the lower

visual areas, but it includes the primary sensory cortex, limbic regions, orbitofrontal cortices, and postcentral gyrus as well. These findings imply an enhanced axonal connection and a higher architectonic similarity in these areas in PBD patients. The ventral pathway of the visual cortex is very closely associated with several other brain regions involved in emotion control. Two studies suggested that functional abnormalities in brain regions associated with the ventral pathway may be involved in the pathophysiological mechanisms occurring in BD (Garrett *et al.*, 2012; Schallmo *et al.*, 2015). It is also plausible that it indicates partial compensation for the network (Duverne *et al.*, 2009; Kloeppel *et al.*, 2015), and could potentially add to exploration of the cellular underpinnings of PBD.

In PBD-related gene analysis, the discovered gene NR1D1 ($r_{(177)} = 0.34$, $P_{FDR} < 0.001$, the highest degree of positive correlation with MSN differences) has been reported to be associated with PBD. It was also reported to be related to circadian rhythms. However, a single genetic variant can have a relatively small effect on complex psychiatric disorders. BD is thought to arise because of multiple loci interacting together and jointly affecting the individual. Interestingly, it was found that the two closely related clock genes RORA and RORB were significantly correlated with the *t*-map (RORA: $r_{(177)} = 0.41$, $p_{FDR} < 0.001$; RORB: $r_{(177)} = 0.32$, $P_{FDR} < 0.001$). The results in this study supported the strong

gene–gene interactions found among genes NR1D1, RORA, and RORB (Lai *et al.*, 2015). Further research is awaited in exploration of the molecular basis behind PBD by understanding the roles encoding proteins play in circadian pathways.

In our research, PLS− gene sets showed specifical enrichment in significantly down-regulated BD-related genes from Gandal *et al.* (2018). However, our results showed that PLS− genes were also enriched in other major psychiatric disorders (e.g. autism spectrum disorder). This might suggest that some prevalent psychiatric diseases share possible convergent pathophysiological processes. (Anttila *et al.*, 2018; Cross-Disorder Group of the Psychiatric Genomics, 2013). It is also worth noting that PBD is a distinct subtype of BD (Faraone *et al.*, 2003; Spencer *et al.*, 2001), and it may have unique genetic underpinnings. Thus, it is necessary to test the specificity of PBD gene enrichments based on more PBD-related studies in the context of neuroimaging transcriptomics.

By introducing 507 negative-weighted genes into Metascape, a topological clustering interaction network that enriched several GO biological processes was obtained. In the obtained GO biological processes, trans-synaptic signaling, which underlies crucial molecular functioning, was noted (de Wit & Ghosh, 2016; Fossati *et al.*, 2019). Disrupted trans-synaptic signaling could impact synapses, which is a significant factor in the pathological basis of BD (Sui *et al.*, 2013). The abnormal regulation of ion transport may be associated with BD (Cherry & Swann, 1994). Those discovered pathways may provide a new direction for developing novel treatments specifically for PBD.

Finally, it was found that excitatory and inhibitory neurons were contributors to dysregulated gene expression in PBD. The PLS analysis of MSN alterations in PBD found that the excitatory neurons accounted for the largest proportion of gene sequences. Unbalanced specification or dysfunction of excitatory and inhibitory neurons in some brain regions is an emerging hypothesis for explaining BD (Lee *et al.*, 2018; Sawada *et al.*, 2020). The determined PBD-related cell types further confirmed the veracity of the specific genes acquired from MSN. It also provided evidence for analyzing and sorting post-mortem brain tissue to find treatments for PBD.

Some limitations in this study should be noted. First, the measurement of AHBA data was based on post-mortem data from six participants with no psychiatric diagnosis. This limitation could lead to insufficiently examined transcriptome–neuroimaging associations between groups. Personal effects might also have been left out of consideration. Furthermore, complete data for the right hemisphere was only collected from two participants. This could lead to insufficient examination of cross-group transcriptome-neuroimaging associations. Moreover, whole-brain data was collected from six adult brains (mean age 43) and not in age-matched participants or patients with PBD (mean age 15). Finally, this study associated MSN phenotypes with genes and cell types. Despite not needing post-mortem brain matter from patients or inferences from model systems, screening for cell types and gene expression based on MSN differences could be better performed to identify molecularly validated anatomical variations in psychiatric patients.

Supplementary Data

Supplementary data are available at *Psychoradiology* online.

Acknowledgments

Conflict of Interest

References

Alexander-Bloch A, Giedd JN, Bullmore ET (2013) Imaging structural co-variance between human brain regions. *Nat Rev Neurosci* **14**:322–36.

Anderson KM, Collins MA, Kong R, *et al.* (2020) Convergent molecular, cellular, and cortical neuroimaging signatures of major depressive disorder. *Proc Nat Acad Sci USA* **117**:25138–49.

Anticevic A, Brumbaugh MS, Winkler AM, *et al.* (2013) Global prefrontal and fronto-amygdala dysconnectivity in bipolar I disorder with psychosis history. *Biol Psychiatry* **73**:565–73.

Antonius D, Prudent V, Rebani Y, *et al.* (2011) White matter integrity and lack of insight in schizophrenia and schizoaffective disorder. *Schizophr Res* **128**:76–82.

Anttila V, Bulik-Sullivan B, Finucane HK, *et al.* (2018) Analysis of shared heritability in common disorders of the brain. *Science* **360**. https://doi.org/10.1126/science.aap8757.

Arnatkeviciute A, Fulcher BD, Bellgrove MA, *et al.* (2021) Where the genome meets the connectome: understanding how genes shape human brain connectivity. *Neuroimage* **244**:118570.

Arnatkeviciute A, Fulcher BD, Fornito A (2019) A practical guide to linking brain-wide gene expression and neuroimaging data. *Neuroimage* **189**:353–67.

Ashburner M, Ball CA, Blake JA, *et al.* (2000) Gene Ontology: tool for the unification of biology. *Nat Genet* **25**:25–9.

Biederman J, Faraone SV, Petty C, *et al.* (2013) Further evidence that pediatric-onset bipolar disorder comorbid with ADHD represents a distinct subtype: results from a large controlled family study. *J Psychiatr Res* **47**:15–22.

Bora E, Fornito A, Yucel M, *et al.* (2010) Voxelwise meta-analysis of gray matter abnormalities in bipolar disorder. *Biol Psychiatry* **67**:1097–105.

Brooks JO, Foland-Ross LC, Thompson PM, *et al.* (2011) Preliminary evidence of within-subject changes in gray matter density associated with remission of bipolar depression. *Psy Res Neuroimag* **193**: 53–5.

Buysse DJ, Reynolds CF 3rd, Monk TH, *et al.* (1989) The Pittsburgh Sleep Quality Index: a new instrument for psychiatric practice and research. *Psychiatry Res* **28**:193–213. https://doi.org/10.1016/0165-1781(89)90047-4.

Cherry L, Swann AC (1994) Cation transport mediated by Na+,K(+)-adenosine triphosphatase in lymphoblastoma cells from patients with bipolar I disorder, their relatives, and unrelated control subjects. *Psychiatry Res* **53**:111–8.

Croarkin PE, Luby JL, Cercy K, *et al.* (2017) Genetic risk score analysis in early-onset bipolar disorder. *J Clin Psychiatry* **78**: 1337–43.

Cross-Disorder Group of the Psychiatric Genomics, C (2013) Identification of risk loci with shared effects on five major psychiatric disorders: a genome-wide analysis. *Lancet* **381**:1371–9.

Darmanis S, Sloan SA, Zhang Y, *et al.* (2015) A survey of human brain transcriptome diversity at the single cell level. *Proc Nat Acad Sci USA* **112**:7285–90.

de Wit J, Ghosh A (2016) Specification of synaptic connectivity by cell surface interactions. *Nat Rev Neurosci* **17**:22–35.

Dimick MK, Cazes J, Fiksenbaum LM, *et al.* (2020) Proof-of-concept study of a multi-gene risk score in adolescent bipolar disorder. *J Affect Disord* **262**:211–22.

Donahue CJ, Sotiropoulos SN, Jbabdi S, *et al.* (2016) Using diffusion tractography to predict cortical connection strength and distance: a quantitative comparison with tracers in the monkey. *J Neurosci* **36**:6758–70.

Duverne S, Motamedinia S, Rugg MD (2009) The relationship between aging, performance, and the neural correlates of successful memory encoding. *Cereb Cortex* **19**:733–44.

Faraone SV, Glatt SJ, Tsuang MT (2003) The genetics of pediatric-onset bipolar disorder. *Biol Psychiatry* **53**:970–7.

Fernandes HM, Cabral J, van Hartevelt TJ, *et al.* (2019) Disrupted brain structural connectivity in Pediatric Bipolar Disorder with psychosis. *Sci Rep* **9**: Article 13638. https://doi.org/10.1038/s41598-019-50093-4.

Forde NJ, O'Donoghue S, Scanlon C, *et al.* (2015) Structural brain network analysis in families multiply affected with bipolar I disorder. *Psy Res Neuroimag* **234**:44–51.

Fornito A, Arnatkeviciute A, Fulcher BD (2019) Bridging the gap between connectome and transcriptome. *Trends Cogn Sci* **23**:34–50.

Fossati M, Assendorp N, Gemin O, *et al.* (2019) Trans-synaptic signaling through the glutamate receptor delta-1 mediates inhibitory synapse formation in cortical pyramidal neurons. *Neuron* **104**:1081–1094.e7.

Gandal MJ, Haney JR, Parikshak NN, *et al.* (2018) Shared molecular neuropathology across major psychiatric disorders parallels polygenic overlap. *Science* **359**:693–7.

Garrett AS, Reiss AL, Howe ME, *et al.* (2012) Abnormal amygdala and prefrontal cortex activation to facial expressions in pediatric bipolar disorder. *J Am Acad Child Adolesc Psychiatry* **51**:821–31.

Glasser MF, Smith SM, Marcus DS, *et al.* (2016) The Human Connectome Project's neuroimaging approach. *Nat Neurosci* **19**:1175–87.

Goldstein BI, Birmaher B (2012) Prevalence, clinical presentation and differential diagnosis of pediatric bipolar disorder. *Isr J Psychiatry Relat Sci* **49**:3–14.

Gong J, Wang J, Chen P, *et al.* (2021) Large-scale network abnormality in bipolar disorder: a multimodal meta-analysis of resting-state functional and structural magnetic resonance imaging studies. *J Affect Disord* **292**:9–20.

Goulas A, Uylings HBM, Hilgetag CC (2017) Principles of ipsilateral and contralateral cortico-cortical connectivity in the mouse. *Brain Structure Function* **222**:1281–95.

Grande I, Berk M, Birmaher B, *et al.* (2016) Bipolar disorder. *Lancet North Am Ed* **387**:1561–72.

Habib N, Avraham-Davidi I, Basu A, *et al.* (2017) Massively parallel single-nucleus RNA-seq with DroNc-seq. *Nat Methods* **14**:955–8.

Han S, Cui Q, Wang X, *et al.* (2020) The anhedonia is differently modulated by structural covariance network of NAc in bipolar disorder and major depressive disorder. *Prog Neuropsychopharmacol Biol Psychiatry* **99**:109865.

Kim S, Kim Y-W, Jeon H, *et al.* (2020) Altered cortical thickness-based individualized structural covariance networks in patients with schizophrenia and bipolar disorder. *J Clin Med* **9**: Article 1846. https://doi.org/10.3390/jcm9061846.

Kloeppel S, Gregory S, Scheller E, *et al.* (2015) Compensation in Pre-clinical Huntington's Disease: evidence from the Track-On HD Study. *eBiomedicine* **2**:1420–9.

Krishnan A, Williams LJ, McIntosh AR, *et al.* (2011) Partial least squares (PLS) methods for neuroimaging: a tutorial and review. *Neuroimage* **56**:455–75.

Lai YC, Kao CF, Lu ML, *et al.* (2015) Investigation of associations between NR1D1, RORA and RORB genes and bipolar disorder. *PLoS ONE* **10**:e0121245.

Lake BB, Chen S, Sos BC, *et al.* (2018) Integrative single-cell analysis of transcriptional and epigenetic states in the human adult brain. *Nat Biotechnol* **36**:70–80.

Lee Y, Zhang Y, Kim S, *et al.* (2018) Excitatory and inhibitory synaptic dysfunction in mania: an emerging hypothesis from animal model studies. *Exp Mol Med* **50**: Article 12. https://doi.org/10.1038/s12276-018-0028-y.

Li J, Seidlitz J, Suckling J, *et al.* (2021) Cortical structural differences in major depressive disorder correlate with cell type-specific transcriptional signatures. *Nat Commun* **12**:1647.

Li M, Santpere G, Imamura Kawasawa Y, *et al.* (2018) Integrative functional genomic analysis of human brain development and neuropsychiatric risks. *Science* **362**. https://doi.org/10.1126/science.aat7615.

Lippard ETC, Jensen KP, Wang F, *et al.* (2017) Effects of ANK3 variation on gray and white matter in bipolar disorder. *Mol Psychiatry* **22**:1345–51.

Maier-Hein KH, Neher PF, Houde JC, *et al.* (2017) The challenge of mapping the human connectome based on diffusion tractography. *Nat Commun* **8**: Article 1349. https://doi.org/10.1038/s41467-017-01285-x.

Morgan SE, Seidlitz J, Whitaker KJ, *et al.* (2019) Cortical patterning of abnormal morphometric similarity in psychosis is associated with brain expression of schizophrenia-related genes. *Proc Natl Acad Sci USA* **116**:9604–9.

Oquendo MA, Ellis SP, Chesin MS, *et al.* (2013) Familial transmission of parental mood disorders: unipolar and bipolar disorders in offspring. *Bipolar Disord* **15**:764–73.

Ou X, Crane DE, MacIntosh BJ, *et al.* (2015) CACNA1C rs1006737 genotype and bipolar disorder: focus on intermediate phenotypes and cardiovascular comorbidity. *Neurosci Biobehav Rev* **55**: 198–210.

Phillips ML, Swartz HA (2014) A critical appraisal of neuroimaging studies of bipolar disorder: toward a new conceptualization of underlying neural circuitry and a road map for future research. *Am J Psychiatry* **171**:829–43.

Rolls ET (2019) The cingulate cortex and limbic systems for emotion, action, and memory. *Brain Structure Function* **224**:3001–18.

Romero-Garcia R, Warrier V, Bullmore ET, *et al.* (2019) Synaptic and transcriptionally downregulated genes are associated with cortical thickness differences in autism. *Mol Psychiatry* **24**:1053–64.

Sawada T, Chater TE, Sasagawa Y, *et al.* (2020) Developmental excitation-inhibition imbalance underlying psychoses revealed by single-cell analyses of discordant twins-derived cerebral organoids. *Mol Psychiatry* **25**:2695–711.

Schallmo MP, Sponheim SR, Olman CA (2015) Reduced contextual effects on visual contrast perception in schizophrenia and bipolar affective disorder. *Psychol Med* **45**:3527–37.

Seidlitz J, Nadig A, Liu S, *et al.* (2020) Transcriptomic and cellular decoding of regional brain vulnerability to neurogenetic disorders. *Nat Commun* **11**. https://doi.org/10.1038/s41467-020-17051-5.

Seidlitz J, Vasa F, Shinn M, *et al.* (2018) Morphometric similarity networks detect microscale cortical organization and predict inter-individual cognitive variation. *Neuron* **97**:231–47 e237.

Selvaraj S, Arnone D, Job D, *et al.* (2012) Grey matter differences in bipolar disorder: a meta-analysis of voxel-based morphometry studies. *Bipolar Disord* **14**:135–45.

Spencer TJ, Biederman J, Wozniak J, *et al.* (2001) Parsing pediatric bipolar disorder from its associated comorbidity with the disruptive behavior disorders. *Biol Psychiatry* **49**:1062–70.

Strakowski SM, Eliassen JC, Lamy M, *et al.* (2011) Functional magnetic resonance imaging brain activation in bipolar mania: evidence for disruption of the ventrolateral prefrontal-amygdala emotional pathway. *Biol Psychiatry* **69**:381–8.

Sui L, Song X-J, Ren J, *et al.* (2013) Intracerebroventricular administration of ouabain alters synaptic plasticity and dopamine release in rat medial prefrontal cortex. *J Neural Transm* **120**:1191–9.

Sunkin SM, Ng L, Lau C, *et al.* (2013) Allen Brain Atlas: an integrated spatio-temporal portal for exploring the central nervous system. *Nucleic Acids Res* **41**:D996–1008.

Vasa F, Seidlitz J, Romero-Garcia R, *et al.* (2018) Adolescent tuning of association cortex in human structural brain networks. *Cereb Cortex* **28**:281–94.

Walton E, Turner J, Gollub RL, *et al.* (2013) Cumulative genetic risk and prefrontal activity in patients with schizophrenia. *Schizophr Bull* **39**:703–11.

Wei Y, Scholtens LH, Turk E, *et al.* (2019) Multiscale examination of cytoarchitectonic similarity and human brain connectivity. *Netw Neurosci* **3**:124–37.

Wood A, Kroll L, Moore A, *et al.* (1995) Properties of the mood and feelings questionnaire in adolescent psychiatric outpatients: a research note. *J Child Psych Psychiat Allied Discip* **36**: 327–34.

Wray NR, Gottesman II (2012) Using summary data from the danish national registers to estimate heritabilities for schizophrenia, bipolar disorder, and major depressive disorder. *Front Genet* **3**:118.

Young RC, Biggs JT, Ziegler VE, *et al.* (1978) A rating scale for mania: reliability, validity and sensitivity. *Br J Psychiatry* **133**:429–35.

Yu M, Linn KA, Cook PA, *et al.* (2018) Statistical harmonization corrects site effects in functional connectivity measurements from multi-site fMRI data. *Hum Brain Mapp* **39**:4213–27.

Zhang X, Gao W, Cao W, *et al.* (2022) Pallidal volume reduction and prefrontal-striatal-thalamic functional connectivity disruption in pediatric bipolar disorders. *J Affect Disord* **301**:281–8.

Zhang Y, Sloan SA, Clarke LE, *et al.* (2016) Purification and characterization of progenitor and mature human astrocytes reveals transcriptional and functional differences with mouse. *Neuron* **89**:37–53.

Zhou Y, Zhou B, Pache L, *et al.* (2019) Metascape provides a biologist-oriented resource for the analysis of systems-level datasets. *Nat Commun* **10**: Article 1523. https://doi.org/10.1038/s41467-019-09234-6.